 CMES, vol.101, no.6, pp.365-386, 2014

A Regularized Method of Fundamental Solutions for 3D and Axisymmetric Potential Problems

Csaba Gáspár[1]

Abstract: The Method of Fundamental Solutions (MFS) is investigated for 3D potential problem in the case when the source points are located along the boundary of the domain of the original problem and coincide with the collocation points. This generates singularities at the boundary collocation points, which are eliminated in different ways. The (weak) singularities due to the singularity of the fundamental solution at the origin are eliminated by using approximate but continuous fundamental solution instead of the original one (regularization). The (stronger) singularities due to the singularity of the normal derivatives of the fundamental solution are eliminated by solving special auxiliary subproblems (desingularization). The desingularization idea is similar to a previously published technique and is completely independent of the applied regularization technique. The presented method produces well-conditioned or moderately ill-conditioned matrices in the resulting linear system of algebraic equations, while the accuracy remains acceptable. No boundary mesh structure is needed. The method is generalized to 3D axisymmetric potential problems in a natural way, despite in this case the fundamental solution does not remain a radial function. The use of extremely ill-conditioned matrices is still avoided.

1 Introduction

Elliptic partial differential equations play an essential role in a lot of fields of application. Modeling stationary phenomena such as diffusion in fluids or in gases, heat transfer, seepage through porous media etc. lead to solving elliptic problems. The usual implicit time discretization techniques of many time-dependent problems result in elliptic problems as well, at every time step. To handle elliptic problems in a meshless way, a number of methods have been developed. A widely spread approach is the Method of Fundamental Solutions [see e.g Alves, Chen, and Šarler (2002)], which is based on the fundamental solution of the applied partial differential operator. These methods are suitable to handle homogeneous problems. For

[1] Széchenyi István University, Győr, Hungary. E-mail: gasparcs@sze.hu

non-homogeneous problems, the approach can be combined with the well-known principle of the Method of Particular Solutions, where the solution is expressed as a sum of a particular solution and a homogeneous solution. These terms can be treated independently and in completely different ways. To calculate a particular solution, a popular technique is the method of radial basis functions (RBFs), which introduces a set of inner interpolation points, but no boundary conditions are prescribed. In contrast to it, the calculation of the homogeneous solution can be performed in a boundary-only way using e.g. the Method of Fundamental Solutions.

In its original form, the MFS produces an approximate solution of the homogeneous equation in the form of a linear combination of the fundamental solutions shifted to external *source points*, where the a priori unknown coefficients have to be calculated by enforcing the boundary conditions at some *boundary collocation points*.

It is well known that the MFS generally produces quite accurate approximate solutions; the accuracy increases further if the source points are located far from the boundary (provided that the exact solution is smooth enough). The price of the excellent accuracy is that the method results in fully populated, nonsymmetric and severely ill-conditioned linear systems; the condition number grows rapidly when the distance of the source points and the boundary increases. In addition to it, for general, non-convex and/or not simply connected domains, the proper locations of the external source points can hardly be automatized. On the other hand, if the source points are loceted close to the boundary, numerical singularities appear in the approximate solution, which destroys the accuracy of the approximation.

To handle the problem of singularity in a meshless way, several methods have been developed. In the Boundary Knot Method [BKM, see Chen (2002); Chen, Shen, Shen, and Yuan (2005)] the solution is approximated by nonsingular general solutions instead of the fundamental solutions. A somewhat similar possibility is to use fundamental solutions concentrated to *lines* rather than discrete points [Gáspár (2013a)]. In both of the above methods , the solution is approximated by nonsingular functions. Unfortunately, though they have excellent accuracy, the resulting linear system is extremely ill-conditioned, which can cause serious computational difficulties.

In MFS-context, when the source and the collocation points coincide, the problem of singularity is always present. It can be circumvented by various tools. In the pioneering work of Young, Chen, and Lee (2005), the solution is approximated by a discretized form of a double layer potential; the singular terms are calculated by extracting the singularities using some simple integral identities. Note, however, that this procedure needs a boundary mesh structure, but less mesh information is

utilized than in the case of the conventional boundary element method. In the Modified Method of Fundamental Solutions [MMFS, see Šarler (2008); Šarler (2009)], the approximate solution is defined by standard boundary element techniques based on single layer and double layer potentials; the appearing regular boundary integrals are evaluated by simple boundary quadrature formulas, while the appearing singular integrals are computed analytically or via auxiliary Dirichlet subproblems. Note again, that for computing the above boundary integrals, a boundary mesh structure is still needed.

The Singular Boundary Method [SBM, see Chen and Wang (2010)] produces the approximate solution in a classical MFS-form, where the source and the collocation points coincide; however, the singular terms are defined with the help of an auxiliary Dirichlet subproblem, where the corresponding collocation points are located *inside* the domain. Thus, the approximate solution still exhibits singularities at the boundary source points; in addition to this, it requires some inner collocation points as well. In its original form, the SBM could handle pure Dirichlet problems. Later, improved versions of the SBM have also been developed to treat Neumann and mixed problems as well [Chen and Gu (2012)]. Here, along the Neumann boundary, the appearing singular terms (called origin intensity factors) are calculated by a similar technique as in Young, Chen, and Lee (2005) based on similar integral identities. Along the Dirichlet boundary, the singular terms are defined by solving an auxiliary Neumann subproblem. This approach needs no interior collocation points, but a boundary mesh structure is still required. The method can be generalized to 3D and more general partial differential equations applied to various physical phenomena [Gu, Chen, and Zhang (2011); Gu, Chen, and He (2012)].

The Boundary Distributed Source method [BDS, see Liu (2010)] uses sources which are not concentrated to discrete source points but they are uniformly distributed in small circles (in 2D problems; the approach can be generalized to 3D problems in a straightforward way). Thus, *regularized* fundamental solutions are obtained, which have no singularity, but satisfy the original partial differential equation outside of small neighbourhoods of the source points only. Consequently, at Dirichlet boundaries, no singular terms appear. Along the Neumann boundaries, the singular terms are calculated by solving an auxiliary pure Dirichlet problem (based on the approach of Šarler (2008)); however, no boundary mesh structure is needed.

In this paper, a similar, but simpler approach is applied. Instead of using the original fundamental solution, regularized fundamental solutions are used, which are defined by truncation or by a singularly perturbed fourth-order partial differential operator. The regularized fundamental solution is continuous at the origin, so that the Dirichlet boundaries can be treated without appearing singularities. Along

the Neumann boundaries, a desingularization technique similar to that of the BDS is applied (based on an auxiliary Dirichlet subproblem). See Gáspár (2013c) for details of the 2D version of the method. Here the method is generalized to 3D potential problems and also to axisymmetric problems. The resulting algebraic systems remain well-conditioned or moderately ill-conditioned, while the accuracy has proved acceptable.

2 The MFS for 3D potential problems

In this section, we restrict ourselves to the 3D Laplace equation:

$$\Delta u = 0 \quad \text{in } \Omega \tag{1}$$

supplied with mixed boundary conditions:

$$u|_{\Gamma_D} = u_D, \quad \frac{\partial u}{\partial n}|_{\Gamma_N} = v_N \tag{2}$$

Here $\Omega \subset \mathbf{R}^3$ is a bounded, sufficiently smooth domain; denote by $\Gamma := \partial\Omega$ the boundary. Assume that Γ is decomposed into a Dirichlet part Γ_D and a Neumann part Γ_N (one of them may be empty). The boundary data u_D, v_N are assumed to be sufficiently regular functions so that the problem (1)-(2) has a unique solution in a proper function space.

The fundamental solution of (1) has the form

$$\Phi(x) = \frac{1}{4\pi||x||}, \tag{3}$$

where $||.||$ denotes the Euclidean norm in $\mathbf{R}^3$. Φ satisfies the equality $\Delta\Phi = -\delta$, where δ is the Dirac distribution concentrated to the origin.

The traditional MFS defines an approximate solution of the problem (1)-(2) in the following form:

$$u(x) \approx \sum_{j=1}^{N} \alpha_j \Phi(x - \tilde{x}_j), \tag{4}$$

where $\alpha_1, ..., \alpha_N$ are a priori unknown coefficients and $\tilde{x}_1, ..., \tilde{x}_N$ are so-called *source points* located outside of the domain Ω. The function defined by (4) is clearly harmonic inside the domain Ω and has singularities at the source points. The coefficients $\alpha_1, ..., \alpha_N$ can be computed by enforcing the boundary conditions at some

collocation points $x_1,...,x_N$ located on the boundary Γ. This results in a linear system of algebraic equations:

$$\begin{aligned}
&\sum_{j=1}^{N} \alpha_j \Phi(x_k - \tilde{x}_j) = u_D(x_k) \qquad (x_k \in \Gamma_D) \\
&\sum_{j=1}^{N} \alpha_j \frac{\partial \Phi}{\partial n_k}(x_k - \tilde{x}_j) = v_N(x_k) \qquad (x_k \in \Gamma_N),
\end{aligned} \tag{5}$$

where n_k denotes the outward normal unit vector at the boundary collocation point x_k.

It is well known that the MFS generally produces quite accurate approximate solutions: the accuracy increases if the source points are located far from the boundary. The price of the accuracy is that the matrix of the system (5) is severely ill-conditioned (and is always fully populated and non-symmetric); the condition number grows rapidly when the distance of the source points and the boundary increases. The system (5) becomes soon so ill-conditioned that it can hardly be solved by the usual methods such as the Gaussian elimination.

In 3D problems, an additional difficulty arises from the high number of source/ collocation points, despite only the boundary Γ has to be discretized by the collocation points (due to the fact that the MFS is a boundary-only method). If the density of the discretization is doubled in each space direction, the number of the boundary collocation points increases by a factor of 4. Thus, using a traditional Gaussian elimination, the number of necessary arithmetic operations increases by a factor of $4^3 = 64$, which may lead soon to severe computational difficulties.

Example 1: To illustrate the above well-known phenomenon, consider the problem (1)-(2) defined on the unit cube $\Omega := (0,1) \times (0,1) \times (0,1)$ with the test solution

$$u(x,y,z) := x^2 + z^2 - 2y^2, \tag{6}$$

where we have used the more familiar notations x,y,z for the space coordinates. Here the edges of the cube were divided into m equal parts, i.e. each side was divided into m^2 congruent subsquares (cells). The boundary collocation points were defined to be the cell centers, so that the total number of boundary collocation points is $N = 6m^2$. The source points were located in the outward normal direction from the collocation points at a distance of $k \cdot h$, where $h := \frac{1}{m}$ denotes the cell size. The left and the right sides of the cube (i.e. for which $y = 0$ and $y = 1$, respectively) were assumed to be Dirichlet boundaries; the Neumann boundary was formed by the remaining four sides. The boundary data were defined to be consistent with the test solution (6). Table 1 shows the relative L_2-errors of the approximate solution defined by the MFS computed on the boundary Γ (in %) with several values of

Table 1: Traditional MFS, Example 1. Test solution: (6). Mixed boundary condition. Relative L_2-errors (%) on the boundary (upper values) and condition numbers (lower values).

$m \setminus k$	1	2	4	8	16	32
2	6.282	1.989	0.5950	0.1857	0.0039	0.0145
	40	371	9.4E+3	5.2E+5	4.4E+7	4.5E+9
4	3.409	0.8877	0.1427	0.0099	3.4E–4	7.9E–6
	185	6.1E+3	2.0E+6	8.2E+9	1.7E+14	2.2E+18
8	2.051	0.4455	0.0475	8.0E–4	1.3E–6	1.2E–6
	588	3.1E+4	7.1E+7	3.9E+13	3.9E+19	6.7E+20
16	1.363	0.2448	0.0223	2.0E–4	1.1E–6	4.9E–7
	1.5E+3	9.9E+4	4.4E+8	5.4E+15	1.5E+20	2.0E+21

the constants m and k defined above (upper values). Table 1 also contains the corresponding condition numbers (lower values).

Remark: In analyzing the accuracy, it is sufficient to compute the error of the approximate solution on the boundary only. Once the boundary values of the function u have been computed, the inner solution can be reconstructed independently by solving a *pure Dirichlet problem*, which is often less difficult from computational point of view than the solution of the original (mixed) problem.

It can clearly be seen that the error decreases rapidly when either the number of source points or their distance from the boundary increases. However, in both cases, the condition numbers very rapidly increase at the same time.

An acceptable compromise seems to locate the source points at a distance of the same order of magnitude as the cell size (i.e. the characteristic distance of the boundary collocation points; see the first and second columns of Table 1).

In most practical cases, however, the discretization of the boundary is not uniform. This is the case especially when a surface mesh has been created by a kind of meshing software (e.g. ANSYS or Nastran). To apply the MFS, there is of course no need to utilize the whole mesh structure. In the next two examples, the surface of Ω was discretized by triangular meshes. The boundary collocation points were defined to be the barycenters of the surface triangles. For each triangle T_j, the radius ρ_j of the inscribed circle was calculated, and the corresponding source point was located in the outward normal direction from the barycenter at a distance of $k \cdot \rho_j$, where k denotes a factor of proportionality. The values of ρ_j characterize the 'local fineness' of the boundary discretization.

Table 2: Traditional MFS, Example 2. Test solution: (6). Mixed boundary condition. Relative L_2-errors (%) on the boundary and condition numbers.

k	1	2	4	8	16
Relative L_2-error (%)	3.094	0.3929	0.0442	0.0030	1.1E–4
Condition number	163	1.2E+3	6.9E+4	2.0E+8	1.7E+16

Example 2: Here the domain Ω is the following cube: $\Omega := (-5,5) \times (-5,5) \times (-5,5)$. The number of surface triangles (thus, the number of boundary collocation points as well as the number of source points) is $N = 1440$. The test solution was again (6). Along the sides, where the y-coordinates of the points are minimal (resp. maximal), i.e. along the left and right sides, Dirichlet boundary condition was prescribed; the remaining boundary points were assumed to be of Neumann type. Table 2 shows the relative L_2-errors of the approximate solution defined by the MFS computed on the boundary Γ (in %) with different values of the factor k. The corresponding condition numbers are also shown. It can be seen again that the farther the source points are located, the more accurate the approximate solution.

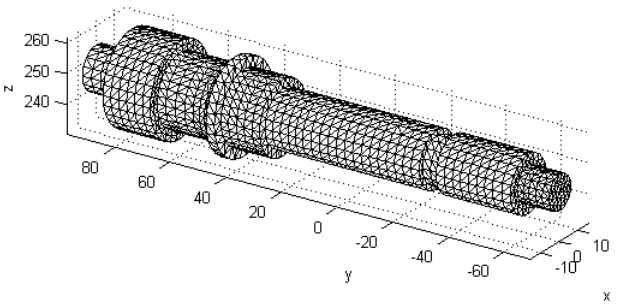

Figure 1: The 3D object in Example 3 with a boundary mesh.

Example 3: Now the domain Ω is more realistic. It is a piece of a hybrid engine (see Figure 1). The shape of the object is axisymmetric (the axis of symmetry is parallel

Table 3: Traditional MFS, Example 3. Axisymmetric domain, test solution: (6). Mixed boundary condition. Relative L_2-errors (%) on the boundary and condition numbers.

k	1	2	4	8	16
Relative L_2-error (%)	74.85	46.86	2.7202	0.1916	7.5E–4
Condition number	112	2.7E+3	5.2E+6	2.7E+11	6.5E+17

with the y-axis). The number of surface triangles is $N = 3318$. The test solution is still (6). Along the sides, where the y-coordinates of the points are minimal or maximal, Dirichlet boundary condition was prescribed. The remaining boundary points were assumed to be of Neumann type. Table 3 shows the relative L_2-errors of the approximate solution defined by the MFS computed on the boundary Γ (in %) with different values of the factor k. The table contains also the corresponding condition numbers. Comparing the results of Table 3 with those of Table 2, it can be seen that the tendency is the same: when the distance of the source points and the boundary increases, the accuracy also increases but the condition number rapidly grows at the same time. However, due to the more complicated geometry, in order that an acceptable accuracy is achieved, the source points should be located at longer distance from the boundary than earlier, which results in much higher condition numbers.

To summarize, if the sources are located far from the boundary, the resulting algebraic system (5) may become severely ill-conditioned, which causes heavy computational problems. In addition to it, if the domain is non-convex, it is difficult to define the locations of the source points in an automatized way. On the other hand, however, if the sources are too close to the boundary, numerical singularities are generated, which destroys the accuracy of the approximation. To eliminate these singularities, special tools are needed. In the next section, some of such techniques are outlined: they are the generalizations of the methods developed originally to handle 2D problems, see e.g. Gáspár (2008), Gáspár (2009), Gáspár (2013c).

3 Regularization and desingularization

In the paper, we use the word 'regularization' when the singularity problems due to the singularity of the fundamental solution (3) are to be avoided. In the presence of Neumann boundary conditions, the normal derivative of the fundamental solution also appears, which has stronger singularity than the fundamental solution itself. To overcome the computational problems arising from the singularity of the nor-

mal derivative of the fundamental solution, other tools (called 'desingularization techniques') are needed.

The simplest regularization technique is the use of truncated fundamental solution

$$\Phi(x) := \begin{cases} \dfrac{1}{4\pi \cdot c \cdot ||x||}, & \text{if } c \cdot ||x|| \geq 1 \\ \dfrac{1}{4\pi}, & \text{if } c \cdot ||x|| < 1 \end{cases} \tag{7}$$

instead of the original fundamental solution $\frac{1}{4\pi \cdot ||x||}$. The positive factor c plays a scaling role and should be defined to be inversely proportional to the characteristic distance of the boundary collocation points, see Gáspár (2008), Gáspár (2013c). It is clear that the function Φ defined by (7) is continuous everywhere; the truncation has influence in a small neighbourhood of the origin only, provided that c is sufficiently large.

Thus, if the problem (1) is supplied with pure Dirichlet boundary condition, then, using the truncated fundamental solution, the source and the collocation points may coincide without generating any singularities. In this case, the approximate solution has the form

$$u(x) \approx \sum_{j=1}^{N} \alpha_j \Phi(x - x_j), \tag{8}$$

and the coefficients $\alpha_1, ..., \alpha_N$ can be computed by enforcing the Dirichlet boundary conditions:

$$\sum_{j=1}^{N} \alpha_j A_{kj} = u_D(x_k) \quad (k = 1, 2, ..., N), \tag{9}$$

where Φ denotes from now on the truncated fundamental solution (7) and

$$A_{kj} := \Phi(x_k - x_j) \qquad (k, j = 1, 2, ..., N) \tag{10}$$

Remarks:

- In fact, the expression (8) results in a radial basis function (RBF) type interpolation function, which approximates the Dirichlet boundary condition u_D along the boundary and is harmonic in Ω apart from a narrow vicinity of the boundary. Roughly speaking, if the boundary approximation is accurate enough, then u remains a good approximation in the whole domain.

- Another strategy for the regularization is to replace the fundamental solution (3) with the fundamental solution of the fourth-order partial differential operator $\Delta\left(I-\frac{1}{c^2}\Delta\right)$, i.e.:

$$\Phi(x)=\frac{1}{4\pi}\cdot\left(-\frac{e^{-c||x||}}{||x||}+\frac{1}{||x||}\right)$$

The scaling parameter c should be again inversely proportional to the characteristic distance of the boundary collocation points. The function Φ approximates the harmonic fundamental solution outside of a small neighbourhood of the origin but remains continuous at the origin (the singularities of the two terms cancel out). This is a 3D generalization of the regularization proposed in Gáspár (2008).

Unfortunately, the approach fails to work in the presence of Neumann boundaries, since the appearing normal derivatives of the fundamental solution have stronger singularity at the collocation points, and the derivatives of the truncated fundamental solution are completely different from those of the original fundamental solution. More precisely, the normal derivative of the approximate solution (8) has the form:

$$\frac{\partial u}{\partial n}(x)\approx\sum_{j=1}^{N}\alpha_j\frac{\partial\Phi}{\partial n}(x-x_j), \tag{11}$$

whence, at Neumann boundaries:

$$\sum_{j=1}^{N}\alpha_j B_{kj}=v_N(x_k)\qquad(x_k\in\Gamma_N) \tag{12}$$

where

$$B_{kj}:=\frac{\partial\Phi}{\partial n_k}(x_k-x_j)\qquad(j\neq k), \tag{13}$$

but the diagonal entries B_{kk} have to be defined in another way called 'desingularization'. To do this, various techniques have been developed, as overviewed in the Introduction, see e.g. Young, Chen, and Lee (2005), Šarler (2008), Šarler (2009), Chen and Wang (2010). Here the idea of Liu (2010) (proposed originally for 2D potential problems) is applied. Consider the auxiliary pure Dirichlet problem

$$\Delta w=0\quad\text{in }\Omega,\qquad w|_\Gamma=1 \tag{14}$$

The exact solution is obviously $w = 1$. Expressing w in the same form as in (8):

$$1 = w(x) \approx \sum_{j=1}^{N} \beta_j \Phi(x - x_j)$$

The coefficients $\beta_1, ..., \beta_N$ can be computed by solving the system

$$\sum_{j=1}^{N} \beta_j A_{kj} = 1 \quad (k = 1, 2, ..., N)$$

Since $\frac{\partial w}{\partial n}$ identically vanishes along the boundary:

$$\sum_{j=1}^{N} \beta_j B_{kj} = \sum_{j \neq k} \beta_j B_{kj} + \beta_k B_{kk} = 0,$$

from which B_{kk} can be defined as:

$$B_{kk} = -\frac{1}{\beta_k} \cdot \sum_{j \neq k} \beta_j B_{kj} \tag{15}$$

Now the method of truncated fundamental solutions can be applied to the mixed problem (1)-(2) as well. The approximate solution is expressed in the form (8), and the a priori unknown coefficients can be computed by solving the linear system:

$$\begin{aligned} &\sum_{j=1}^{N} \alpha_j A_{kj} = u_D(x_k) \quad (x_k \in \Gamma_D) \\ &\sum_{j=1}^{N} \alpha_j B_{kj} = v_N(x_k) \quad (x_k \in \Gamma_N), \end{aligned} \tag{16}$$

Remarks:

- The diagonal element B_{kk} is well defined by Eq. (15) provided that β_k differs from zero. If not, other particular solutions (possibly several ones) can also be used; Eq. (15) is rewritten as:

$$B_{kk} = \frac{1}{\beta_k} \cdot \left(\frac{\partial w}{\partial n_k}(x_k) - \sum_{j \neq k} \beta_j B_{kj} \right)$$

- Similar desingularization techniques appear also in other methods such as the Modified Method of Fundamental Solutions (MMFS, see Šarler (2008),

Šarler (2009)); the Singular Boundary Method (SBM, see Gu, Chen, and Zhang (2011), Chen and Gu (2012) for 2D problems and also Gu, Chen, and He (2012) for 3D problems), and so forth. Note, however, that the above technique needs no boundary mesh structure at all, similarly to the Boundary Distributed Source method (see Liu (2010))

- The above desingularization technique can be improved by redefining not only the singular diagonal elements of the matrix B but also the 'quasi-singular' neighbouring elements, using more auxiliary Dirichlet problems, see Gáspár (2013b) for the 2D version of the method. The technique can be generalized for 3D problems in a straightforward way. However, this requires information on the neighbouring boundary collocation points, which can be easily achieved if a boundary mesh structure is given. Otherwise, this requires some additional preprocessing task, which, however, does not increase the computational complexity by a significant amount.

- The desingularization techniques can be defined for the *dipole formulation* as well, when the approximate solution is defined by the form

$$u(x) \approx \sum_{j=1}^{N} \alpha_j \frac{\partial \Phi}{\partial n_j}(x - x_j).$$

From a computational point of view, the dipole formulation has proved more advantageous than the above outlined monopole formulation for pure Dirichlet problems, while for pure Neumann problems, the monopole formulation overperforms the dipole formulation resulting in much less condition numbers (at least in the case of 2D problems, see Gáspár (2014)). Utilizing this observation, the mixed problems can be converted to a sequence of pure Dirichlet and pure Neumann subproblems, the solutions of which converge rapidly to the solution of the original mixed problem but require much less computational cost. See Gáspár (2014) for details.

Example 4: Consider again the problem (1)-(2) with the test solution (6). The domain Ω is the unit cube $\Omega := (0,1) \times (0,1) \times (0,1)$, and the faces are divided into m^2 congruent subsquares (cells). The source and the boundary collocation points are defined to be the cell centers. Two opposite sides are defined to be of Dirichlet type, the remaining sides form the Neumann boundary. Table 4 shows the relative L_2-errors of the approximate solution (based on regularization and desingularization defined above) computed on the boundary Γ (in %) with several values of the constant m and the scaling constant c. The table contains also the corresponding condition numbers (lower values). The results clearly show that the optimal value

Table 4: Truncated MFS, Example 4. Test solution: (6). Mixed boundary condition. Relative L_2-errors (%) on the boundary (upper values) and condition numbers (lower values).

$m \setminus c$	4	8	16	32	64	128
2	35.15	2.071	68.07	208.9	491.7	1057.9
	20.0	6.0	2.5	2.9	5.4	10.9
4	131.0	18.65	0.6774	35.61	108.3	254.7
	656.3	83.6	13.7	5.3	2.5	3.7
8	41.88	15.75	9.069	0.1553	18.35	55.33
	1.8E+4	1.6E+5	209.2	29.2	11.3	5.2
16	40.48	13.35	6.105	4.365	0.1060	9.262
	3.4E+6	2.7E+5	4.4E+4	441.5	60.5	23.5

Table 5: Truncated MFS, Example 5. Test solution: (6). Mixed boundary condition. Relative L_2-errors (%) on the boundary and condition numbers.

k	1.00	1.25	1.50	1.75	2.00	2.25
Relative L_2-error (%)	6.270	3.9899	1.670	0.6876	3.039	5.407
Condition number	155.9	75.7	50.1	37.6	30.1	25.1

of the scaling parameter is inversely proportional to the characteristic distance of the boundary collocation points.

Example 5: The test problem as well as the boundary conditions remain the same as in Example 4, but here we have a triangular surface mesh introduced in Example 2 ($\Omega := (-5,5) \times (-5,5) \times (-5,5)$, the mesh consists of 1440 non-congruent triangles, the barycenters of which play the role of the boundary collocation points). Here we applied scaling factors c_j varying from triangle to triangle defined as

$$c_j := k \cdot \frac{1}{\rho_j},$$

where k is a factor of proportionality and ρ_j denotes again the radius of the inscribed circle belonging to the jth triangle. Table 5 shows the relative L_2-errors of the approximate solution (based on regularization and desingularization defined above) computed on the boundary Γ (in %) with some different values of the factor k as well as the corresponding condition numbers.

Table 6: Truncated MFS, Example 6. Axisymmetric domain, test solution: (6). Mixed boundary condition. Relative L_2-errors (%) on the boundary and condition numbers.

k	1.25	1.50	1.75	2.00
Relative L_2-error (%)	0.3559	0.2460	0.2284	0.4846
Condition number	5.8E+5	289.8	363.7	722.0

Example 6: Now the domain was replaced with the axisymmetric domain described in Example 3. The same surface mesh was used (the mesh consists of 3318 non-congruent triangles; the boundary collocation points are defined to be their barycenters). The scaling factors c_j are defined exactly as in Example 5. Table 6 shows the relative L_2-errors and the corresponding condition numbers with some different values of the factor k.

From Tables 5 and 6, it can be seen that the factor k should be defined to be approximately $1.50 \ldots 1.75$, which results in acceptable accuracy in both cases though the domain in Example 6 is much more complicated than in Example 5. In addition to it, the system (16) remains well-conditioned in contrast to the traditional version of the MFS shown in Tables 1-3.

4 Axisymmetric problems

If both the domain Ω and the boundary data have axial symmetry, the original 3D problem can be reduced to a 2D one:

$$\Delta u = \frac{1}{r}\frac{\partial}{\partial r}\left(r \cdot \frac{\partial u}{\partial r}\right) + \frac{\partial^2 u}{\partial z^2} = \frac{\partial^2 u}{\partial r^2} + \frac{1}{r} \cdot \frac{\partial u}{\partial r} + \frac{\partial^2 u}{\partial z^2} = 0, \tag{17}$$

where we used the more familiar cylindrical coordinates r, z, and, without loss of generality we assumed that the axis of symmetry is the z-axis.

The domain of Equation (17) is now lies on the upper half-plane (i.e. $r > 0$ for each point (r,z) of Ω). The boundary of Ω (still denoted by Γ) consists of a Dirichlet part Γ_D and a Neumann part Γ_N. However, due to the axial symmetry, the intersection of the boundary and the z-axis can be omitted from Γ since a homogeneous Neumann boundary condition is automatically satisfied here. Along the remaining part, mixed boundary condition is prescribed:

$$u|_{\Gamma_D} = u_D, \quad \frac{\partial u}{\partial n}|_{\Gamma_N} = v_N \tag{18}$$

The axisymmetric potential Φ_A generated by a point source at (r_0, z_0) can be obtained by integrating a single layer potential concentrated to a circle with center $(0, z_0)$ and radius r_0 over this circle which implies (apart from a multiplicative constant):

$$\Phi_A(r, z, r_0, z_0) = \frac{4}{R} \cdot K(\kappa), \tag{19}$$

(see Karageorghis and Fairweather (1999)), where K denotes the complete elliptic integral of the first kind:

$$K(x) := \int_0^1 \frac{1}{\sqrt{1-t^2} \cdot \sqrt{1-x^2t^2}}\, dt = \int_0^{\pi/2} \frac{1}{\sqrt{1-x^2 \sin^2\theta}}\, d\theta,$$

where $0 \le x < 1$, and R, κ are defined as follows:

$$R := \sqrt{(r+r_0)^2 + (z-z_0)^2}, \quad \kappa := \frac{2 \cdot \sqrt{r \cdot r_0}}{R}.$$

The function defined by (19) is considered a fundamental solution of (17). As a function of r and z, Φ_A solves Equation (17) everywhere, except for the point (r_0, z_0).

The problem of singularity appears again. If $r \to r_0$, $z \to z_0$, then obviously $\kappa \to 1$ and $\Phi(r, z, r_0, z_0) \to +\infty$. More precisely, using the well-known asymptotic expansion formula of the complete elliptic integrals:

$$K(1-x) = \log 2\sqrt{2} - \frac{1}{2} \log x + \mathcal{O}(|x \cdot \log x|),$$

one can easily deduce that, if $r \to r_0$, $z \to z_0$:

$$\Phi_A(r, z, r_0, z_0) = \frac{4}{R} \log \sqrt{8R(R + 2\sqrt{r r_0})} - \frac{4}{R} \log d + \mathcal{O}(d \cdot |\log d|),$$

where $d := \sqrt{(r-r_0)^2 + (z-z_0)^2}$. This means, that, as expected, Φ has a logarithmic singularity at the point (r_0, z_0).

Note that (19) is *not* a radial function, however, from this point, the main ideas of the MFS can be utilized without difficulty.

Let (r_j, z_j) (resp. $(\tilde{r}_j, \tilde{z}_j)$) be boundary collocation (resp. source) points ($r_j, \tilde{r}_j > 0$), where the source points are located outside of the domain Ω. Then the solution of (17)-(18) can be approximated in the form:

$$u(r, z) \approx \sum_{j=1}^{N} \alpha_j \cdot \Phi_A(r, z, \tilde{r}_j, \tilde{z}_j), \tag{20}$$

where the coefficients α_j can be determined by enforcing the boundary conditions:

$$\begin{aligned}
&\sum_{j=1}^{N} \alpha_j \Phi_A(r_k, z_k, \tilde{r}_j, \tilde{z}_j) = u_D(r_k, z_k) \quad ((r_k, z_k) \in \Gamma_D) \\
&\sum_{j=1}^{N} \alpha_j \frac{\partial \Phi_A}{\partial n_k}(r_k, z_k, \tilde{r}_j, \tilde{z}_j) = v_N(r_k, z_k) \quad ((r_k, z_k) \in \Gamma_N),
\end{aligned} \tag{21}$$

Note, however, that the calculation of the derivatives of Φ_A is not trivial. Denote by E the complete elliptic integral of the second kind:

$$E(x) := \int_0^1 \frac{\sqrt{1-x^2t^2}}{\sqrt{1-t^2}}\, dt = \int_0^{\pi/2} \sqrt{1-x^2\sin^2\theta}\, d\theta$$

Using the well-known equalities for the derivatives of the complete elliptic integrals:

$$K'(x) = -\frac{K(x)}{x} + \frac{E(x)}{(1-x^2)\cdot x}$$

$$E'(x) = -\frac{K(x)}{x} + \frac{E(x)}{x},$$

after some calculations, the derivatives of Φ_A can be determined (see Karageorghis and Fairweather (1999)), yielding:

$$\begin{aligned}
\frac{\partial \Phi_A}{\partial r} &= -\frac{2}{rR}\cdot K(\kappa) + \frac{2(-r^2 + r_0^2 + (z-z_0)^2)}{rR((r-r_0)^2 + (z-z_0)^2)}\cdot E(\kappa) \\
\frac{\partial \Phi_A}{\partial z} &= -\frac{4(z-z_0)}{R((r-r_0)^2 + (z-z_0)^2)}\cdot E(\kappa)
\end{aligned} \tag{22}$$

Remark: Direct calculations show that

$$\frac{\partial \Phi_A}{\partial r} = \frac{2}{R\cdot((r-r_0)^2 + (z-z_0)^2)}\cdot$$

$$\cdot\left(-(K(\kappa)+E(\kappa))r + 2K(\kappa)r_0 + \frac{-K(\kappa)+E(\kappa)}{r}\cdot(r_0^2 + (z-z_0)^2)\right)$$

Hence, using the well-known asymptotic expansion formulas of the complete elliptic integrals

$$K(x) = \frac{\pi}{2} + \frac{\pi}{8}x^2 + \mathcal{O}(x^4),$$

$$E(x) = \frac{\pi}{2} - \frac{\pi}{8}x^2 + \mathcal{O}(x^4),$$

it follows that

$$\lim_{r\to 0} \frac{\partial \Phi_A}{\partial r}(r,z,r_0,z_0) = 0$$

(with $r_0 > 0$). This means that the normal derivative of the fundamental solution Φ_A, as a function of r and z, vanishes along the z-axis. Thus, the approximate solution (20) automatically satisfies a homogeneous Neumann boundary condition along the intersection of the boundary and the z-axis, as expected.

4.1 Regularization and desingularization

Since Φ_A has a logarithmic singularity at the point (r_0, z_0) a regularization technique is needed. The truncation applied in the previous section is not quite straightforward due to the fact that Φ_A is not a radial function. First define a truncation for the function κ. By definition:

$$\kappa^2 = \frac{4rr_0}{(r+r_0)^2 + (z-z_0)^2},$$

whence

$$1 - \kappa = \frac{1-\kappa^2}{1+\kappa} = \frac{(r-r_0)^2 + (z-z_0)^2}{R(R+2\sqrt{rr_0})}$$

which implies that

$$\kappa = 1 - \frac{(r-r_0)^2 + (z-z_0)^2}{R(R+2\sqrt{rr_0})}$$

Now let $c > 0$ be a scaling factor, and, instead of κ, use the following redefined function (still denoted by κ):

$$\kappa(r,z,r_0,z_0) :=$$

$$:= \begin{cases} 1 - \dfrac{(r-r_0)^2 + (z-z_0)^2}{R(R+2\sqrt{rr_0})}, & \text{if } (r-r_0)^2 + (z-z_0)^2 > \dfrac{1}{c^2} \\ 1 - \dfrac{1}{R(R+2\sqrt{rr_0})} \cdot \dfrac{1}{c^2}, & \text{if } (r-r_0)^2 + (z-z_0)^2 \le \dfrac{1}{c^2} \end{cases}$$

Observe that this function is continuous everywhere in the upper half-plane i.e. for $r > 0$, $r_0 > 0$. Clearly, the values of κ do not exceed the value 1. On the other hand, κ is always nonnegative provided that $r_0 \ge \frac{1}{c}$. Indeed, since $R \ge r + r_0$, therefore

$$c^2 R(R+2\sqrt{rr_0}) \ge c^2(r+r_0)\cdot(r+r_0+2\sqrt{rr_0}) \ge c^2 r_0^2 \ge 1,$$

which implies the statement.

Consequently, with this 'truncated' function κ, the 'truncated' fundamental solution

$$\Phi_A(r,z,r_0,z_0) := \frac{4K(\kappa(r,z,r_0,z_0))}{c \cdot R} \tag{23}$$

is well-defined and has no singularity at (r_0,z_0).

The scaling parameter should be defined as earlier: it should be inversely proportional to the characteristic distance of the boundary collocation points. Moreover, the condition $cr_j \geq 1$ should also be satisfied for each boundary collocation point (r_j,z_j).

With this modified function Φ_A defined by (23), the approximate solution of (17)-(18) has the form:

$$u(r,z) \approx \sum_{j=1}^{N} \alpha_j \Phi_A(r,z,r_j,z_j), \tag{24}$$

where the a priori unknown coefficients α_1, ...,α_N can be computed by solving the linear system:

$$\begin{aligned} &\sum_{j=1}^{N} \alpha_j A_{kj} = u_D(x_k) \quad (x_k \in \Gamma_D) \\ &\sum_{j=1}^{N} \alpha_j B_{kj} = v_N(x_k) \quad (x_k \in \Gamma_N), \end{aligned} \tag{25}$$

Here the matrix entries are as follows:

$$A_{kj} := \Phi_A(r_k,z_k,r_j,z_j)$$

$(k,j = 1,2,...,N)$. Moreover, based on the formulas (22), the matrix entries

$$B_{kj} := \frac{\partial \Phi_A}{\partial n_k}(r_k,z_k,r_j,z_j)$$

can also be calculated except for the diagonal entries B_{kk}. To define the diagonal terms, a desingularization process defined in the previous section can be applied based on the particular solution $w = 1$ (or, possibly, on other particular solutions of the axisymmetric Laplace equation).

Example 7: Let Ω be the following rectangle of the (z,r)-plane: $\Omega := (-1,1) \times (0,1)$. A rotation around the z-axis results in a cylinder, the axis of which is the z-axis. Consider the test function:

$$u(r,z) := r^2 - 2z^2, \tag{26}$$

Table 7: Regularized axisymmetric MFS, Example 7. Test solution: (26). Mixed boundary condition. Relative L_2-errors (%) on the boundary (upper values) and condition numbers (lower values).

$N(M) \setminus c$	8	16	32	64	128	256	512
12 (8)	19.44	12.10	42.67	73.18	103.5	133.9	164.2
	6.5	5.2	5.6	6.3	7.0	7.7	8.5
24 (16)	26.57	10.55	5.190	20.82	36.42	51.98	67.52
	52.8	22.9	15.8	12.7	11.0	10.0	9.3
48 (32)	21.31	12.89	5.237	2.551	10.36	18.19	26.03
	402.8	181.0	62.7	40.8	31.6	26.6	23.6
96 (64)	-	9.046	6.325	2.558	1.291	5.172	9.070
	-	3.7E+3	488.1	151.2	94.7	71.6	59.3
192 (128	-	-	4.985	3.136	1.257	0.6532	2.579
	-	-	5.9E+3	1.1E+3	340.3	207.9	154.6
384 (256)	-	-	-	1.709	1.563	0.6228	0.3287
	-	-	-	9.3E+4	2.6E+3	735.5	442.2

which obviously satisfies (17). Along the boundary of Ω, N boundary collocation points are located in an equidistant manner; however, the points lying on the z-axis are not taken into account as boundary collocation points, since the approximate solution (24) automatically satisfies a homogeneous Neumann boundary condition along the intersection of the boundary and the z-axis, as pointed out earlier. The number of the remaining boundary collocation points is denoted by M, while c denotes the scaling factor in (23). At the boundary points for which the z-coordinate is minimal or maximal, i.e. along the left and right sides, Dirichlet boundary condition was prescribed, while the remaining boundary points were assumed to be of Neumann type. Table 7 shows the relative L_2-errors of the approximate solution (24) computed on the boundary (in %) with several values of N and c (upper values). Table 7 also contains the corresponding condition numbers (lower values). The results indicate again that the scaling parameter c should be inversely proportional to the characteristic distance of the boundary collocation points. The missing elements of Table 7 correspond to the situation when the condition $r_j \geq \frac{1}{c}$ is not fulfilled for some j due to the fact that $\frac{1}{c}$ is not small enough, therefore the evaluation of the function κ results in negative values, thus, the evaluation of the elliptic integrals fails.

Example 8: Consider the axisymmetric domain of Examples 3 and 6; the axis of

Table 8: Regularized axisymmetric MFS, Example 8. Test solution: (26). Mixed boundary condition. Relative L_2-errors (%) on the boundary and condition numbers.

k	1.0	3.0	5.0	7.0	9.0
Relative L_2-error (%)	18.75	1.112	0.4812	1.360	5.152
Condition number	1.9E+5	1.0E+3	1.2E+3	1.5E+3	2.5E+3

symmetry is the z-axis. The applied surface mesh consists of 3318 non-congruent triangles again. The z,r-coordinates of the barycenters of the surface triangles defines 3318 boundary points on the (z,r)-plane (some of them might coincide) From these points, a much smaller subset of boundary points was selected using a criterion that the distance of the selected points should exceed a predefined value ε. The scaling factor varied from point to point defined as follows:

$$c_j := k \cdot \frac{1}{\rho_j}$$

where k is a factor of proportionality and ρ_j is the minimal distance between the jth boundary collocation point and the remaining boundary collocation points.

In this example the value of ε was set to $\varepsilon := 0.25$, which resulted in $N = 167$ boundary points. Along the side where the z-coordinate of the points were minimal or maximal, Dirichlet boundary condition was prescribed; the remaining part of the boundary points was treated as Neumann boundary points. Table 8 shows the relative L_2-errors of the approximate solution (20) computed on the boundary (in %) with some different values of the factor k. Table 8 contains the corresponding condition numbers as well. The results show that the method produces acceptable accuracy; the algebraic system (25) is much smaller than in 3D case and remains moderately well-conditioned.

5 Summary and Conclusions

A regularized version of the Method of Fundamental Solutions has been developed for 3D potential problems. The source and boundary collocation points were assumed to coincide. This causes singularities, which have been eliminated by several techniques. The singularities caused by the singularity of the original fundamental solution has been avoided by using a truncated (or other approximate) fundamental solution controlled by a carefully chosen scaling constant. The stronger singularities caused by the Neumann boundary condition i.e. the normal derivatives

of the fundamental solution have been eliminated by a special desingularization technique based on an auxiliary subproblem supplied with pure Dirichlet boundary condition. This results in acceptable accuracy while the problem of the severely ill-conditioned matrices is avoided. The approach has been extended to 3D axisymmetric problems as well, using a truncation technique for the complete elliptic integrals which appear in the fundamental solution of the axisymmetric Laplace operator.

Acknowledgement: The research was partly supported by the European Union (co-financed by the European Social Fund) under the project TÁMOP-4.2.2.A-11/1/KONV-2012-0012.

References

Alves, C. J. S.; Chen, C. S.; Šarler, B. (2002): The method of fundamental solutions for solving Poisson problems. *Int. Series on Advances in Boundary Elements. (Proceedings of the 24th International Conference on the Boundary Element Method incorporating Meshless Solution Seminar). Eds: C.A.Brebbia A.Tadeu, V.Popov, Vol. 13. WitPress, Southampton, Boston*, pp. 67–76.

Chen, W. (2002): Symmetric boundary knot method. *Engineering Analysis with Boundary Elements*, vol. 26, pp. 489–494.

Chen, W.; Gu, Y. (2012): An improved formulation of singular boundary method. *Advances in Applied Mathematics and Mechanics*, vol. 4, no. 5, pp. 543–558.

Chen, W.; Shen, L. J.; Shen, Z. J.; Yuan, G. W. (2005): Boundary Knot Method for Poisson Equations. *Engineering Analysis with Boundary Elements*, vol. 29, pp. 756–760.

Chen, W.; Wang, F. Z. (2010): A Method of Fundamental Solutions Without Fictitious Boundary. *Engineering Analysis with Boundary Elements*, vol. 34, pp. 530–532.

Gáspár, C. (2008): A Multi-Level Regularized Version of the Method of Fundamental Solutions. *The Method of Fundamental Solutions – A Meshless Method. Eds: C.S.Chen, A.Karageorghis, Y.S.Smyrlis, Dynamic Publishers, Inc., Atlanta, USA*, pp. 145–164.

Gáspár, C. (2009): Several Meshless Solution Techniques for the Stokes Flow Equations. *Progress on Meshless Methods. Eds: A.J.M.Ferreira, E.J.Kansa, G.E.Fasshauer. Computational Methods in Applied Sciences*, vol. 11, pp. 141–158.

Gáspár, C. (2013a): A Regularized Method of Fundamental Solutions Without Desingularization. *Computer Modeling in Engineering & Sciencess*, vol. 92, no. 1, pp. 103–121.

Gáspár, C. (2013b): Combining Regularization and Desingularization Techniques in the Method of Fundamental Solutions. *Advances in Boundary Element and Meshless Techniques XIV. ed. by A.Sellier and M.H.Aliabadi. EC Ltd, Eastleigh, England*, vol. 92, no. 1, pp. 103–121.

Gáspár, C. (2013c): Regularization Techniques for the Method of Fundamental Solutions. *Int. J. of Computational Methods*, vol. 10, no. 2, pp. 1341004–1 – 1341004–21.

Gáspár, C. (2014): A Regularized Multi-Level Technique for Solving Potential Problems by the Method of Fundamental Solutions. *Engineering Analysis with Boundary Elements*. In press, doi: 10.1016/j.enganabound.2014.05.002.

Gu, Y.; Chen, W.; He, X. Q. (2012): Singular boundary method for steady-state heat conduction in three dimensional general anisotropic media. *International Journal of Heat and Mass Transfer*, vol. 55, no. 17–18, pp. 4837–4848.

Gu, Y.; Chen, W.; Zhang, C. Z. (2011): Singular boundary method for solving plane strain elastostatic problems. *International Journal of Solids and Structures*, vol. 48, no. 18, pp. 2549–2556.

Karageorghis, A.; Fairweather, G. (1999): The method of fundamental solutions for axisymmetric potential problems. *Int J Numer Meth Engng*, vol. 44, pp. 1653–1669.

Liu, Y. J. (2010): A new boundary meshfree method with distributed sources. *Engineering Analysis with Boundary Elements*, vol. 34, pp. 914–919.

Šarler, B. (2008): A modified method of fundamental solutions for potential flow problems. *The Method of Fundamental Solutions – A Meshless Method. Eds: C.S.Chen, A.Karageorghis, Y.S.Smyrlis, Dynamic Publishers, Inc., Atlanta, USA*, pp. 299–326.

Šarler, B. (2009): Solution of Potential Flow Problems by the Modified Method of Fundamental Solutions: Formulations with the Single Layer and the Double Layer Fundamental Solutions. *Engineering Analysis with Boundary Elements*, vol. 33, pp. 1374–1382.

Young, D. L.; Chen, K. H.; Lee, C. (2005): Novel meshless method for solving the potential problems with arbitrary domain. *Journal of Computational Physics*, vol. 209, pp. 290–321.